Journal of Power Sources 182 (2008) 599–602

Contents lists available at ScienceDirect

Journal of Power Sources

journal homepage: www.elsevier.com/locate/jpowsour

Short communication

Shunt current calculation of fuel cell stack using Simulink®

Jeremy A. Schaeffer[a], Lea-Der Chen[a,*], James P. Seaba[b]

[a] Department of Mechanical and Industrial Engineering, 3131 Seamans Center, The University of Iowa, Iowa City, IA 52242, USA
[b] ConocoPhillips Company, 420 S. Keeler Avenue, Bartlesville, OK 74004, USA

ARTICLE INFO

Article history:
Received 2 March 2008
Received in revised form 3 April 2008
Accepted 4 April 2008
Available online 14 April 2008

Keywords:
Fuel cell stack
Electrolyzer stack
Shunt current
Protective current

ABSTRACT

Presence of shunt current in fuel cell stacks can lead to corrosion and power loss problems. The objective of this paper is to develop a stack-level model for calculation of shunt currents. The simulation model was based on electrical circuit, and created using Simulink® software. The Simulink® results were validated by using PSpice® software and comparing with experimental data of an electrolyzer stack. The Simulink® model is also used to evaluate the effectiveness of a protective current method to reduce the shunt current. The protective current method was found to effectively reduce shunt current of a 100-cell stack. The Simulink® model also shows that shunt current is highest at end cells of the 100-cell stack examined, suggesting extra care be applied to end cells for corrosion prevention. Monte Carlo simulation was performed to examine sensitivity of variance in voltage, manifold, channel and cell resistance on calculated shunt current. The sensitivity analysis shows that calculated shunt current is most sensitive to variance in manifold resistance and followed by variance in voltage, electrolyte and channel resistance. The calculated power loss due to shunt current is within 1% for the conditions examined.

1. Introduction

A fuel cell is an electrochemical device that converts chemical energy stored in the fuel to electrical work. Individual fuel cells are often connected in series to meet voltage requirements of intended applications. When liquid electrolyte is used, for example, in phosphoric acid fuel cells [1] and alkaline fuel cells [2], electrolyte in individual fuel cells is shared through a common manifold, and shunt current may be present [1–9]. Shunt current, also known as bypass current [3], current leakage [4], or parasitic current [6], may be present through the common electrolyte due to presence of the conductive paths and non-zero electrical field potential gradient. Similarly, shunt current may also be present when liquid water is used as coolant in polymer electrolyte fuel cell stacks. Presence of shunt current is not desired because it can lead to fuel cell corrosion and power loss problems.

Corrosion might occur in iron–water systems through electrochemical redox reactions [10]. Acid environment is present in phosphoric acid fuel cells. It might also be present in low temperature polymer electrolyte fuel cells when flooding occurs. Base environment is present in alkaline fuel cells. The voltage-pH equilibrium diagrams of iron–water systems reported in [10] suggest that corrosion may occur in fuel cell stacks when stainless steel is used as separator or manifold materials. Shunt current can also be present when impurities or ions exist in cooling water that circulates through bipolar plates of the fuel cell stack.

Models are developed to predict shunt currents [3–9], for example, in common manifolds and in bipolar plates. Shunt current can be reduced by increasing the electrical resistance of the channels and manifold. This can be accomplished by decreasing the cross-sectional area and increasing the length in the channels and manifold, or decreasing the resistance in the cell. The cell resistance can be decreased by increasing the area of the electrodes and decreasing the distance between the electrodes. However, they will also result in an undesired increase of the pressure drop of the electrolyte flow. Another method to reduce the shunt current is to apply protective current that counters the electrical voltage gradient in the manifold [11]. The power level of applied protective current is usually negligible when compared to fuel cell power output.

The objective of this paper is to develop a stack-level model for calculation of the shunt current distribution in fuel cell stacks. An electrical circuit model is used to simulate the electrical process of liquid electrolyte fuel cell stacks. The calculation is compared with experimental data of an electrolyzer stack reported in [11].

2. Electrical circuit

Shunt current can be modeled [11] using electrical circuit shown in Fig. 1, where R_e is the electrolyte resistance of individual cells, R_c the channel resistance, and R_m is the manifold resistance. A small

* Corresponding author. Tel.: +1 319 335 5674; fax: +1 319 384 0576.
E-mail address: ldchen@engineering.uiowa.edu (L.-D. Chen).

0378-7753/$ – see front matter © 2008 Elsevier B.V. All rights reserved.
doi:10.1016/j.jpowsour.2008.04.014

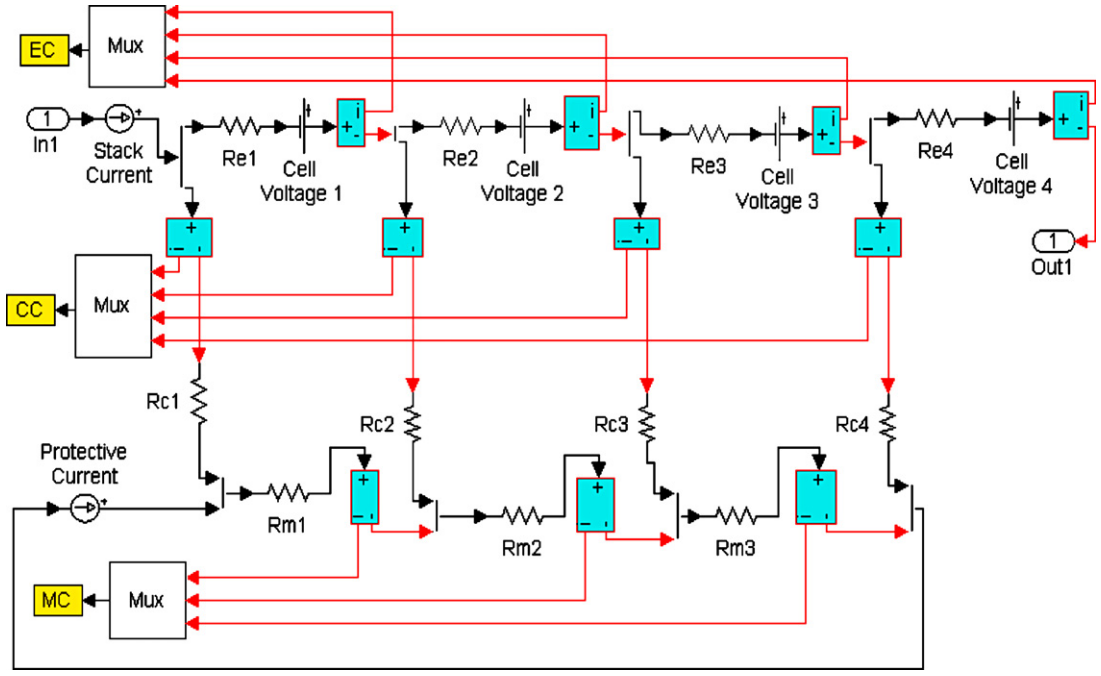

Fig. 1. Illustration of a Simulink® model for four-cell stack, protective current applied to the manifold.

amount of current, or shunt current, will flow through the channel and manifold, resulting in power loss and possibly corrosion problems in manifold. To apply protective current to eliminate the shunt current, the voltage drop through the manifold ($k_0 R_m$) must be the same as the voltage drop through the electrolyte (IR_e). When this condition is met, there will not be a voltage gradient between the cell and manifold. Consequently, no shunt current will flow through the channels. Zahn et al. [11] derived an analytical expression for the protective current, k_0, which assumes the following form:

$$k_0 = \frac{V_0 + IR_e}{R_m} \tag{1}$$

To verify Eq. (1), a Simulink® [12] model is established for the electrical circuit of a four-cell stack shown in Fig. 1. The Simulink® model determines the current flowing through the cells, channels, and manifold using the following parameters: R_e, R_c, R_m, V, I, and k_0. Simulation is run using a Matlab® function [12], and analysis is performed to obtain the following quantities:

$$\mathrm{SC_{abs}} = \sum_{i=1}^{n} |(\mathrm{CC})_i| \tag{2}$$

$$\mathrm{PL} = \frac{|P_{\mathrm{ideal}} - P|}{P_{\mathrm{ideal}}} \tag{3}$$

$$P_{\mathrm{ideal}} = nI^2 R_e \tag{4}$$

$$P = \sum_{i=1}^{n} (\mathrm{EC})_i V - k_0 V \tag{5}$$

Eq. (2) calculates the magnitude of the sum of shunt current in the channels, in which i denotes the channel number and n the total number of the channels. When protective current is applied, the calculated value of $\mathrm{SC_{abs}}$ is a measure of the effectiveness of Eq. (1) to eliminate shunt current. Eq. (3) calculates the percent power loss due to shunt current, where P_{ideal} is the ideal power, i.e., the power level when there is no shunt current present that is calculated by Eq. (4). Eq. (5) calculates the actual power delivered from the stack, P, i.e., the cell power delivered less power required by protective current.

PSpice® software [13] was used to validate Simulink® results. The model parameters used in the calculation were provided by R.J. Bellows, and set to $n = 4$, $R_e = 0.2\ \Omega$, $R_c = 150\ \Omega$, $R_m = 50\ \Omega$, $V = 1$ V, and $I = 1$ A. Electrical current calculated by Simulink® and PSpice® was in agreement to eighth decimal point in mA without protective current, and to sixth decimal point with protective current. Detailed comparison can be found in [14]. The four-stack model is modified for calculation of the 10-cell stack electrolyzer of Zahn et al. [11] and expanded for calculation of a 100-cell fuel cell stack.

3. Results and discussion

The shunt current results of the Simulink® stack model are compared with experimental data of the 10-cell electrolyzer stack reported in [11]. The electrolyzer dimensions were provided by R.J. Bellows, which had an electrode area of 968 mm^2 (1.5 in.^{2}). The distance between the electrodes is estimated to be 31.75 mm (1.25 in.). Based on electrolyte conductivity of 0.15 $\Omega\,\mathrm{cm}^{-1}$ [14], the channel, manifold, and electrolyte resistance is estimated to be 1000, 150, and 2.187 Ω, respectively. The cell voltage is set to 2.54 V with applied current of 420 mA. The experimental results had precision error of either ±0.39 mA or ±1 mA, depending on whether the range selector of the current meter was set to 10 or 30 mA full scales. Experimental data with no protective current are summarized in Fig. 2, in which error bar denotes precision error of ±1 mA. Also shown in the figure are the Simulink® results. The simulation was in general agreement with experimental data and bounded by experimental uncertainty, except for the end channels, channels 1 and 10. The calculated shunt current in channels 1 and 10 was below experimental data by 31%. The simulation also shows a small positive shunt current in channel 5, while a small negative shunt current was recorded in the experiment. The recorded negative current was within experimental uncertainty of ±1 mA.

Simulation results of experiments with protective current of 17.5 mA are summarized in Fig. 3. Simulation shows that shunt current leaves from first half of the cells (i.e., channels 1 through 5) and

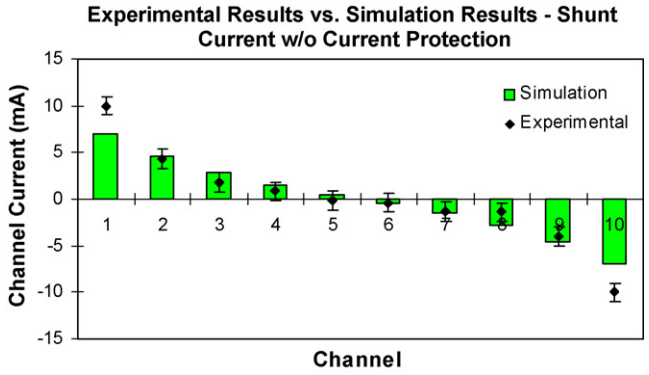

Fig. 2. Comparison of simulation and experimental shunt current without protective current: $R_e = 2.187\,\Omega$, $R_m = 150\,\Omega$, $R_c = 1000\,\Omega$, $V = 2.54\,V$, $I = 0.42\,A$; Error bars ± 1 mA.

returns to second half of the stack (cf., channels 6 through 10). The magnitude of calculated shunt current decreased from end channels toward central channels and was negative symmetric between channels 1 and 10, 2 and 9, 3 and 8, 4 and 7, and 5 and 6. Shunt current was very difficult to measure as suggested by error bars in Fig. 3. Experimental data lack the negative-symmetry characteristic required by theoretical considerations, suggesting further investigations are needed to resolve the differences between simulation and measurements.

To estimate uncertainty in measurements due to variance in resistance of manifold, channel and cell electrolyte, and voltage, Monte Carlo simulation was performed. Monte Carlo simulation with sample sizes of 5000, 10,000, 15,000 and 20,000 were reported in Schaeffer [14]. The histogram based on sample size of 15,000 is somewhat different from that based on sample sizes of 5000 or 10,000, but it is nearly the same as that based on sample size of 20,000. The results presented herein are based on sample size of 15,000, unless specified otherwise. In simulation, a standard deviation of 5% of the mean value was applied to manifold resistance, channel resistance, and cell voltage. Setting variance to 5% is somewhat arbitrary; however, it represents the 95% confidence level that was used to determine experimental uncertainty. Two sets of results were examined in Schaeffer [14]: one was for the conditions without protective current and the other with. The results with protective current will be emphasized in this paper.

The histogram of the results with variance applied to manifold resistance shows that channel shunt currents varied in the range of ± 0.3 to ± 0.4 mA. There also existed a non-zero finite probability of channel current to reverse its direction in channels 5 and 6, and to a lesser degree, in channels 4 and 7. When variance was applied

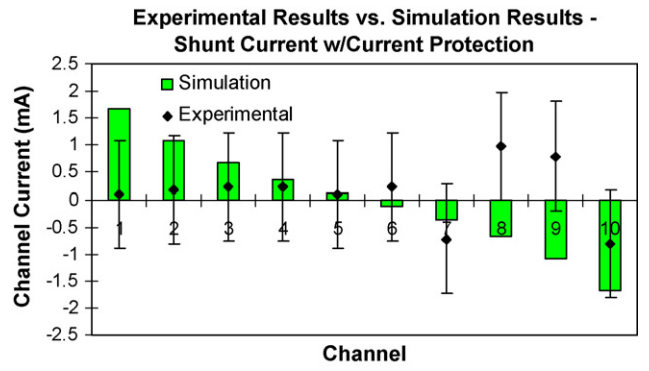

Fig. 3. Comparison of simulation and experimental shunt current with protective current; $R_e = 2.187\,\Omega$, $R_m = 150\,\Omega$, $R_c = 1000\,\Omega$, $V = 2.54\,V$, $I = 0.42\,A$, $I_p = 0.0175\,A$.

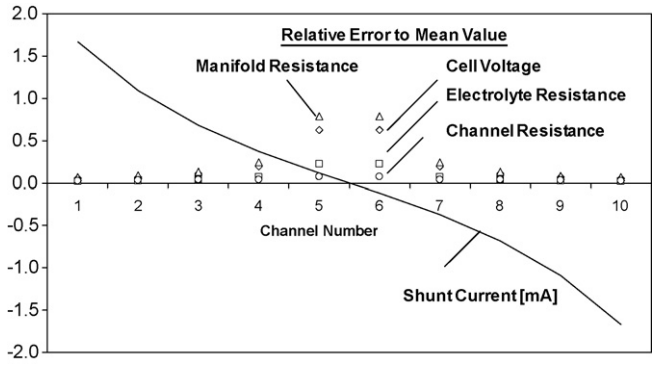

Fig. 4. Relative error of calculated shunt currents as compared to the mean values of the conditions with standard deviation of 5% of the mean applied to voltage (diamond symbol), manifold (triangle symbol), electrolyte (square symbol) and channel (circle symbol) resistance, respectively; the shunt current in mA is also shown (solid line); protective current applied.

to channel resistance, the channel current was seen to vary in the range of ± 0.03 mA for central channels and ± 0.1 or ± 0.15 mA for end channels [14]. No reversed current was predicted. When variance was applied to electrolyte, the resultant variations in channel shunt current were fairly constant, having a value in the range of ± 0.10 to ± 0.15 mA. There was a small non-zero finite probability of channel current flow reversing directions in channel 6. Simulation with protective current was also performed to evaluate the effects of voltage variations. Simulation shows that the resultant variations in channel current are fairly constant, at a level of approximately ± 0.3 mA. A non-zero finite probability of channel current reversing the direction was predicted for channels 5 and 6 and channels 4 and 7 (with a lower probability value). Multiple variances were applied in Monte Carlo simulation and qualitatively similar results were obtained and reported in [14].

Sensitivity analysis based on Monte Carlo simulation was performed to examine how variances in voltage and resistance of manifold, channel, and cell electrolyte impact calculated shunt current. Sample size of 30,000 was used. Fig. 4 summarizes the resultant error due to 5% variance in cell voltage, manifold resistance, electrolyte resistance, and channel resistance, respectively. Variance in manifold resistance results in highest shunt current differences across all channels, followed by variance in voltage, electrolyte resistance, and channel resistance. The largest differences occurred in channels 5 and 6 where shunt currents were lowest (as shown in Fig. 4). The results with simultaneous variations of voltage, manifold resistance, electrolyte resistance, and channel resistance are summarized in Fig. 5. Again, manifold variance dom-

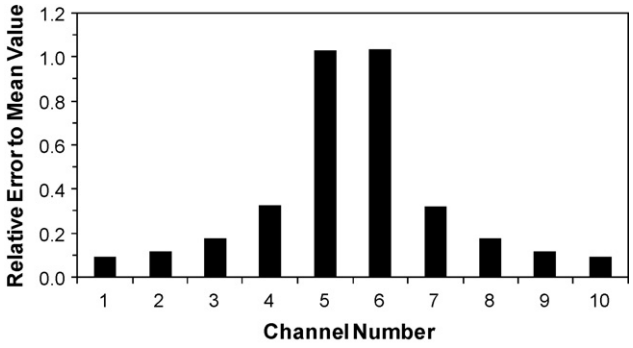

Fig. 5. Relative error of calculated shunt currents as compared to the mean values of the conditions with standard deviation of 5% of the mean applied simultaneously to voltage, manifold, electrolyte, and channel resistance.

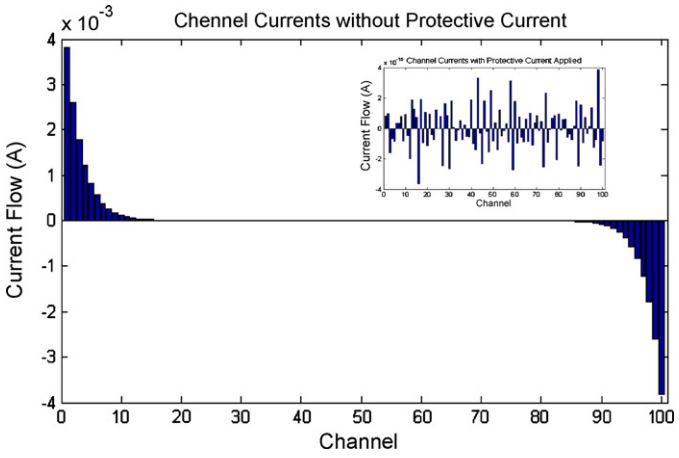

Fig. 6. Shunt current of a 100-cell fuel cell stack.

inates the shunt current calculation. The calculated absolute shunt current, SC_{abs}, is 7.9 mA and corresponding power loss, PL, is 0.65%.

To test the effectiveness of the protective current (Eq. (1)) proposed by Zahn et al. [11], the shunt current calculation is extended to a hypothetical alkaline fuel cell stack of 100 cells. The resistance is set to 75 Ω for each manifold segment, 500 Ω for each channel, and 0.25 Ω for each cell [14], which assumes separator thickness of 1.2 cm, manifold length of 9.0 cm, channel length of 0.6 m, and electrolyte conductivity of 194 mS cm^{-1}. To calculate the wetted areas, current output from single cells is set to 1 A and current density is assumed to be 40 mA cm^{-2}. The resulting wetted areas for separator, channel and manifold are 25, 0.61, and 0.61 cm^2, respectively. The cell voltage, 0.65 V, was estimated based on EIS model parameters of [15]. The calculation shows that the overall shunt current is 23.9 mA and corresponding power lost is 1.13% of delivered power. The shunt current distribution across the 100 cells is summarized in Fig. 6, showing that shunt current decreases from end cells to central cells. The results suggest that end cells of the stack would experience greater risks of corrosion problems. When protective current of 12.0 mA is applied, shunt current in all channels is reduced to a negligible level, 10^{-15} A—lending support to robustness of Eq. (1).

4. Summary and conclusions

A fuel cell stack model for calculation of shunt current in a fuel cell stack was created using Simulink®, and the results were validated by PSpice®. The simulation results were also validated by comparing experimental data of an electrolyzer stack, which was operated with or without the presence of protective current [11]. When no protective current was applied, the simulation results compared well with experimental data. The agreement is generally within experimental uncertainty, except for two end channels. When protective current is applied, less satisfactory agreement was obtained. However, discrepancies were generally within experimental uncertainty, except for three end channels. The protective current proposed by Zahn et al. [11], i.e., that of Eq. (1) is validated by the Simulink®-based fuel cell stack model considered in this paper. Monte Carlo simulation was performed to examine how variance in voltage, manifold, channel, and cell resistance can impact the stack performance. Standard deviation at 5% of the mean was applied. Major findings of the current study are

(1) The protective current proposed by Zahn et al. [11], cf., Eq. (1), can effectively reduce shunt current in the 100-cell stack under the conditions examined in this paper.
(2) The Simulink® model results showed that highest shunt current was present at end cells of a 100-cell stack, suggesting that end cells are more prone to corrosion problems.
(3) The Monte Carlo simulation-based sensitivity analysis shows that calculated shunt current is most sensitive to variance in manifold resistance and followed by variance in voltage, electrolyte, and channel resistance.
(4) The calculated impact of shunt current on power loss is about 1% for the conditions examined.
(5) Significant differences are observed between measurements and simulation for the protective current case shown in Fig. 3. Further investigations are needed to resolve the differences.

Acknowledgments

The authors wish to acknowledge helpful discussions with Dr. R. Bellows, particularly on experimental parameters, and Dr. Yong Miao for the results presented in Figs. 4 and 5. LDC and JPS also wish to acknowledge many helpful discussions with Dr. Pat Grimes, who passed away in 2007.

References

[1] M. Katz, J. Electrochem. Soc. 125 (1978) 515–520.
[2] G.F. McLean, T. Niet, S. Prince-Richard, N. Djilali, Int. J. Hydrogen Energy 27 (2002) 507–526.
[3] R.E. White, C.W. Walton, H.S. Bunney, R.N. Beaver, J. Electrochem. Soc. 133 (1986) 485–492.
[4] H.S. Burney, R.E. White, J. Electrochem. Soc. 133 (1986) 1609–1612.
[5] H.N. Seiger, J. Electrochem. Soc. 133 (1986) 2002–2007.
[6] G. Bonvin, Ch. Comninellis, J. Appl. Electrochem. 24 (1994) 469–474.
[7] S.K. Rangarajan, V. Yegnanarayanan, Electrochim. Acta 42 (1997) 153–165.
[8] S.K. Rangarajan, V. Yegnanarayanan, M. Muthukumar, Electrochim. Acta 44 (1998) 491–502.
[9] E.R. Henqtuin, J.M. Bisang, J. Appl. Electrochem. 35 (2005) 1183–1190.
[10] T.P. Hoar, in: M. Pourbaix (Ed.), Atlas of Electrochemical Equilibrium in Aqueous Solution, Second English Ed., National Association of Corrosion Engineers, Houston, 1974, p. 88.
[11] M. Zahn, P.G. Grimes, R.J. Bellows, Shunt Current Elimination and Device, U.S. Patent no. 4,197,169 (1980).
[12] Simulink®, The MathWorks®, Natick, Massachusetts, http://www.mathworks.com/products/simulink/.
[13] PSpice®, Cadence, San Jose, California, http://www.cadence.com/orcad/index.html.
[14] J.A. Schaeffer, Electrical Circuit Modeling of Fuel Cells, MS Thesis, Department of Mechanical and Industrial Engineering, The University of Iowa, Iowa City, IA, 2004.
[15] H. Dumont, P. Los, L. Brossard, H. Menard, J. Electrochem. Soc. 141 (1994) 1225–1231.